Supplementary Information

## Supplementary Figures:

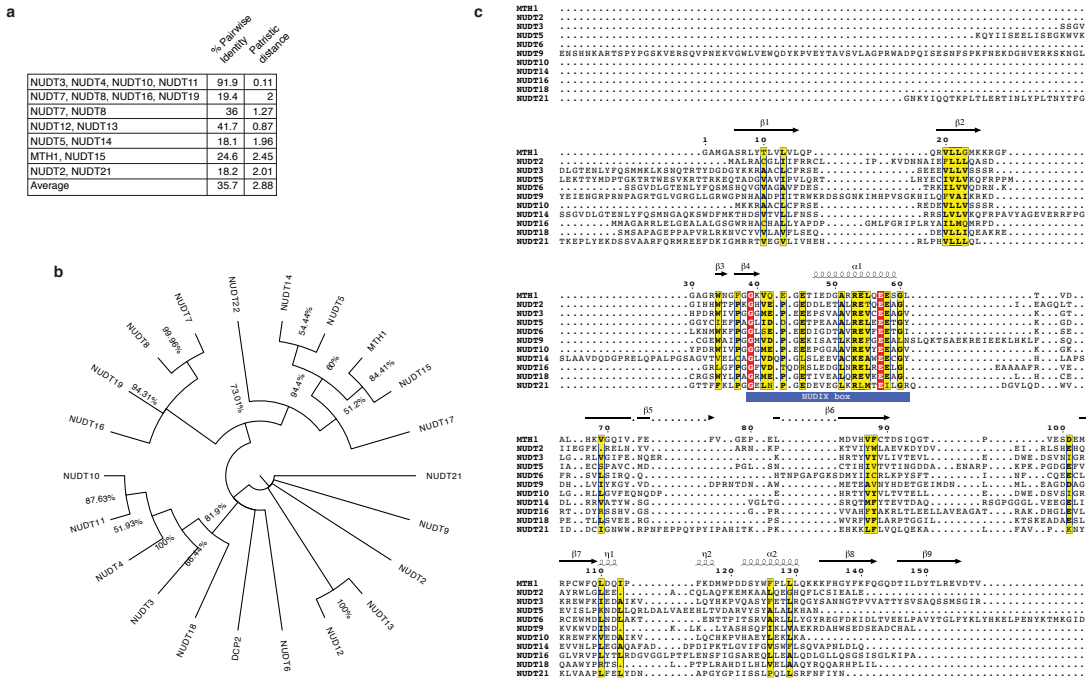


Supplementary Figure 1

**Supplementary Figure 1:** A. % Pairwise distances and Patristic distances for each branch of the consensus phylogenetic tree of NUDIX full length sequences of the human NUDIX enzymes. B. Consensus phylogenetic tree of NUDIX fold sequences of the human NUDIX proteins with % pairwise distances of each branch provided. B**.** Sequence alignment of human NUDIX hydrolases with known structure, homology is highlighted in yellow, strict sequence conservation in red, and the NUDIX box is indicated in blue.

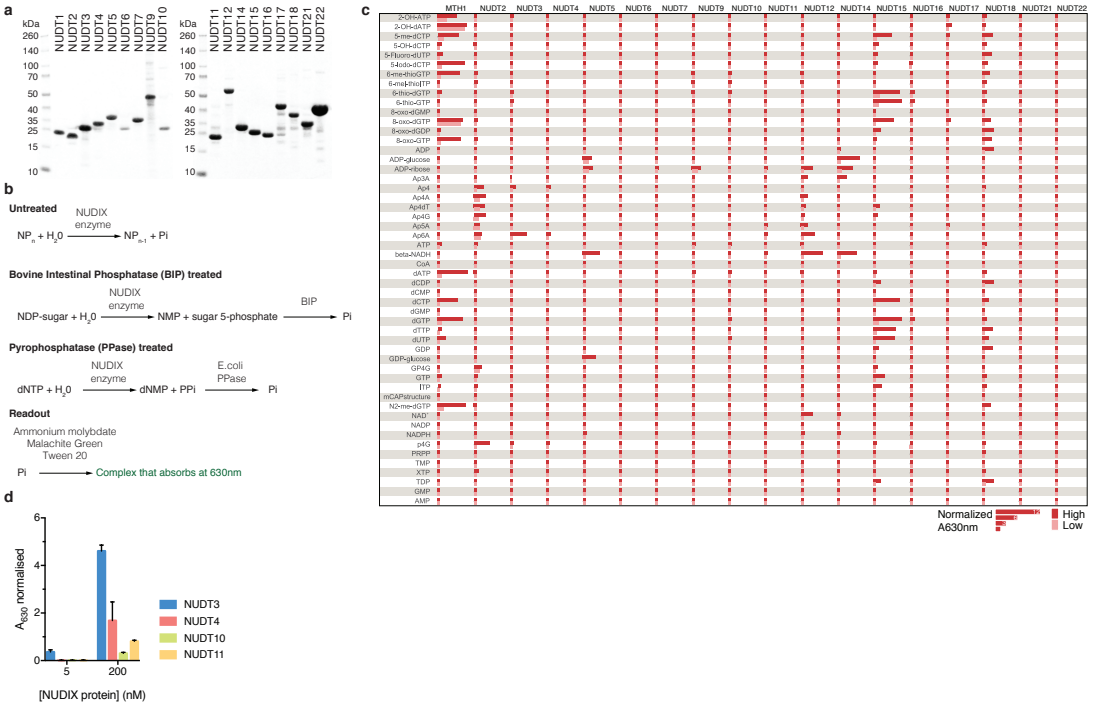


Supplementary Figure 2

**Supplementary Figure 2: NUDIX enzymes purification, substrate screen principle and DIPPs activity.** A: 4 $\mu$g of purified NUDIX protein was analyzed on SDS-PAGE and stained using Coomassie Blue. B: Principles behind the substrate screen, which uses the Malachite Green reaction as read-out. C: Activity of NUDT3, NUDT4, NUDT10 and NUDT11 with 5-PP-InsP5 as substrate. D: Activity of 18 human NUDIX hydrolases towards 52 substrates. Activity is represented by a column bar graph in which the absorbance at 630nm normalized to untreated controls (this is, without BIP or PPase) is shown. Light-red bars indicate activity in conditions of low enzyme concentrations (5 nM), while dark-red bars indicate activity at high enzyme concentration (200 nM).

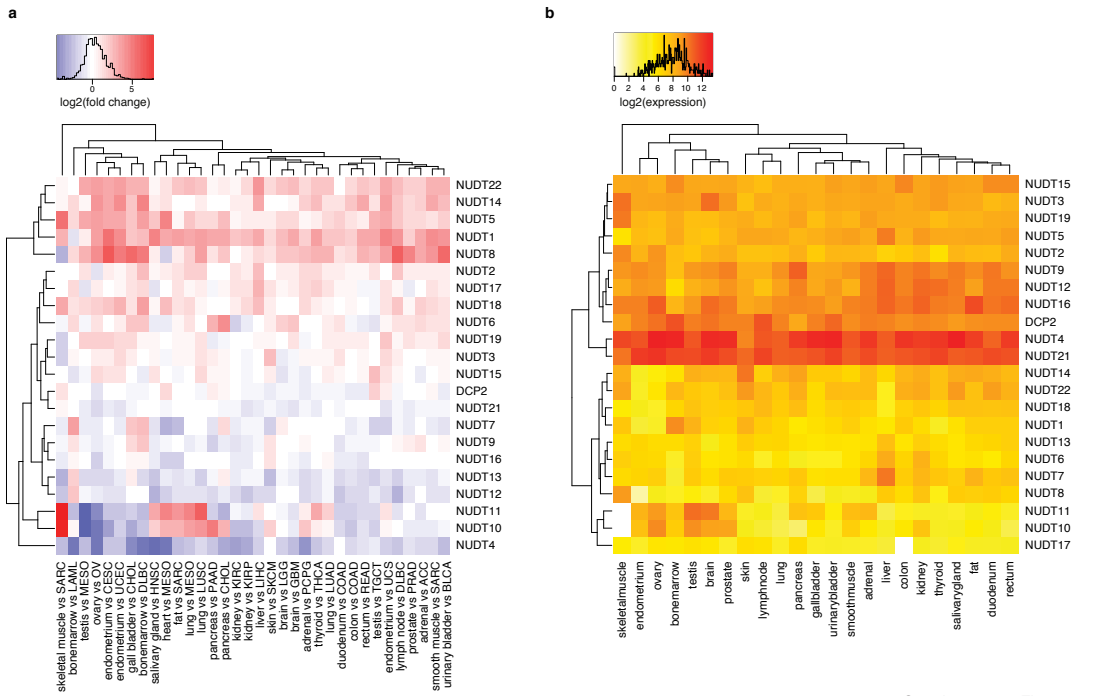


Supplementary Figure 3

**Supplementary Figure 3:** A: Clustering of the NUDIX hydrolases by mRNA expression by comparing normal tissues with their cancer counterparts. B: Clustering of the NUDIX hydrolases by their mRNA expression in normal tissues.

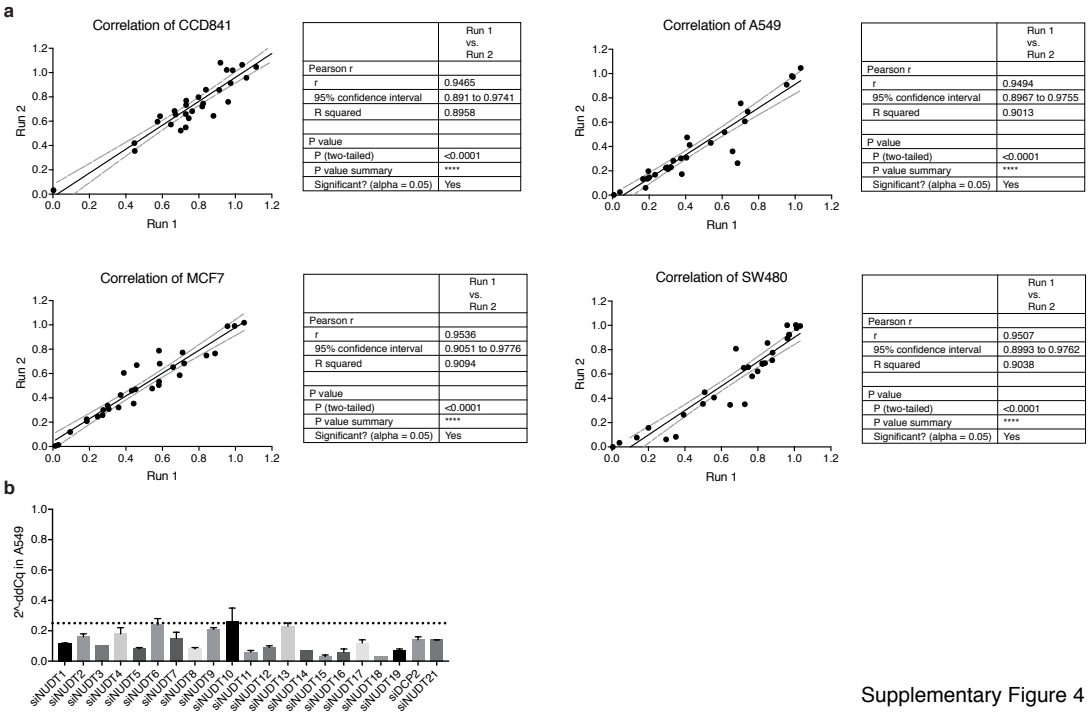


Supplementary Figure 4

**Supplementary Figure 4:** A: Statistical correlation between two independent siRNA knockdown experiments per cell line. B: mRNA expression of the different human NUDIX genes upon siRNA-mediated depletion, measured by qRT-PCR in intra-assay triplicates.

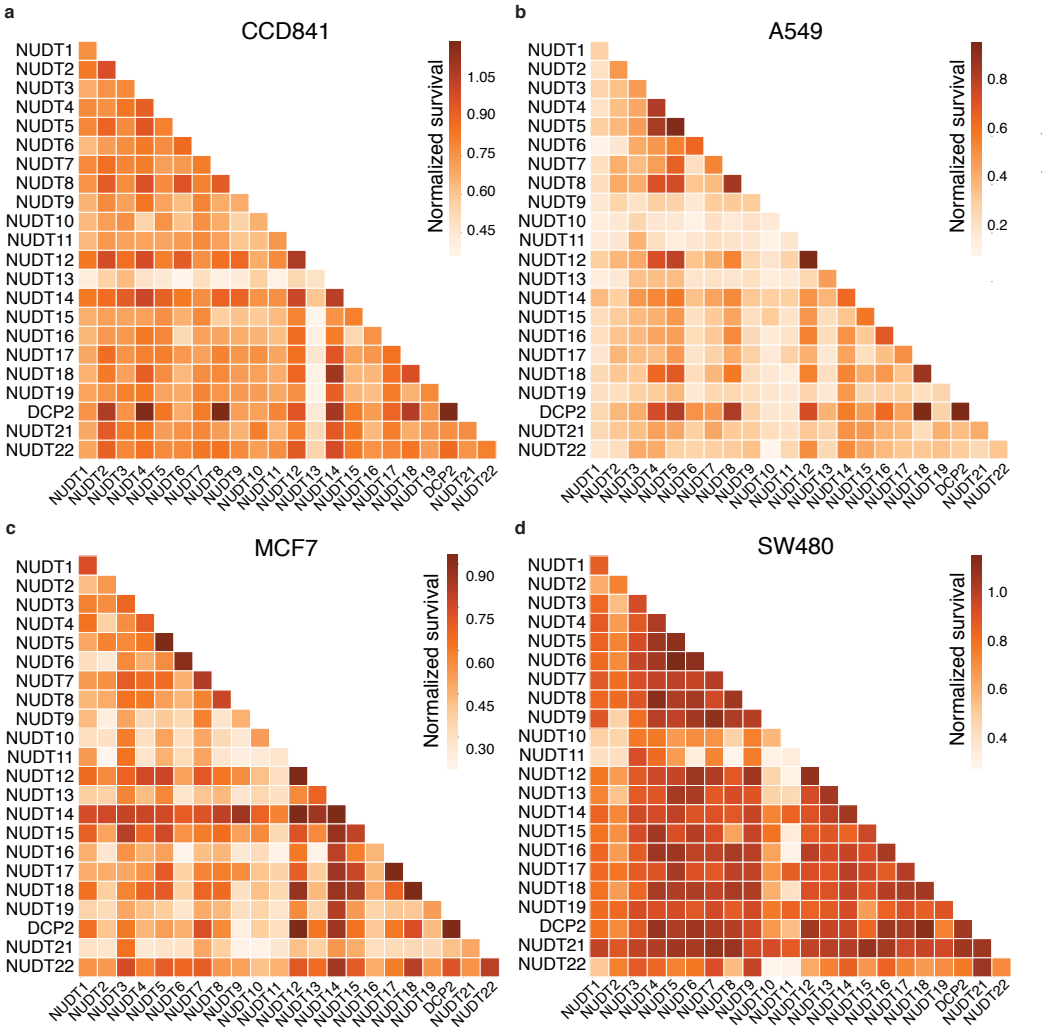


Supplementary Figure 5

**Supplementary Figure 5:** Quantitative scores for cell viability of double NUDIX knockdowns corresponding to (a) CCD841, (b) A549, (c) MCF7 and (d) SW480 respectively and normalized to the corresponding single knockdown.

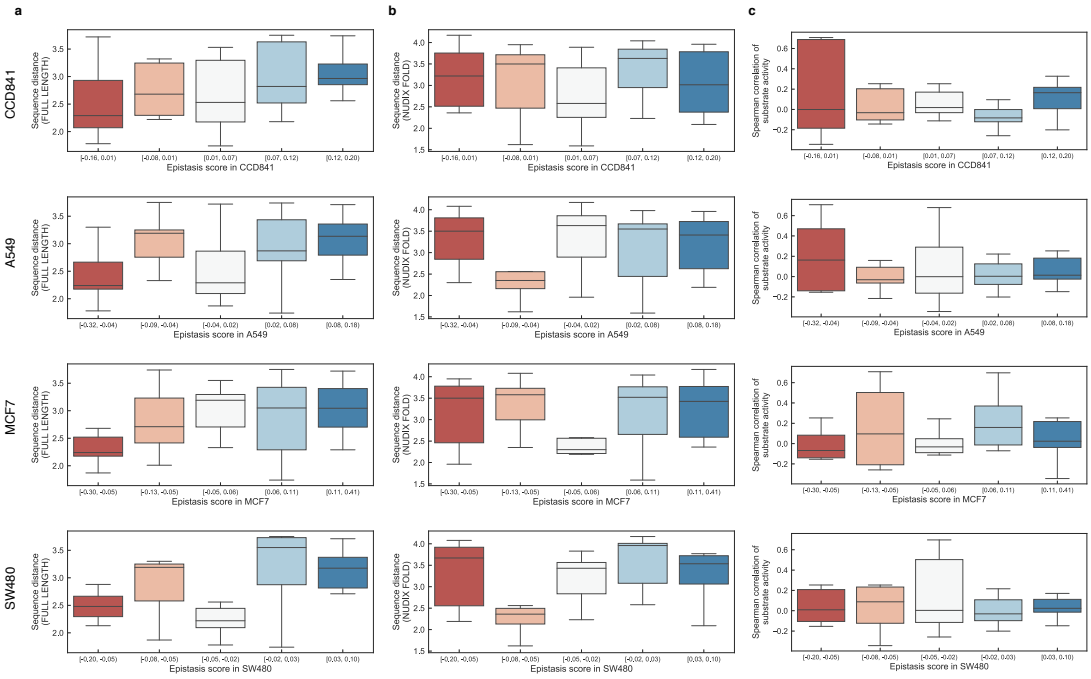


Supplementary Figure 6

**Supplementary Figure 6:** A: Box plot comparing Sequence Patristic distance of full length NUDIX sequence with epistasis scores. B: Box plot comparing Sequence Patristic distance of NUDIX fold sequence with epistasis scores. C: Box plot comparing Spearman rank correlation of substrate activity similarity with epistasis scores.

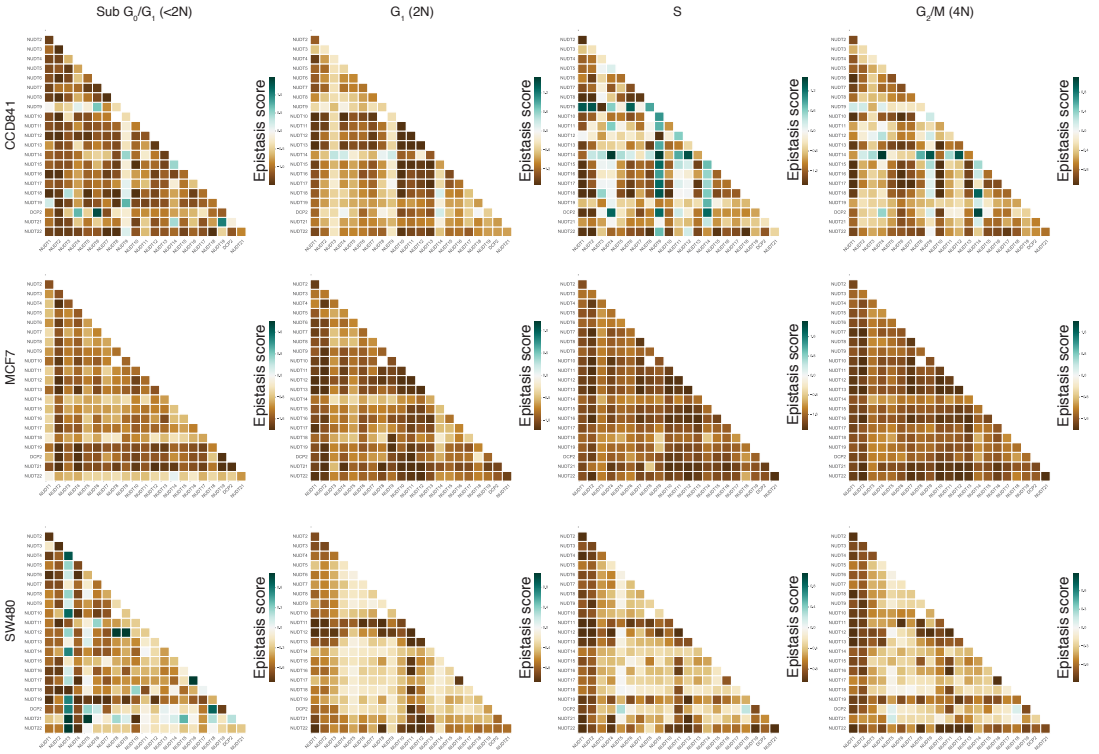


Supplementary Figure 7

**Supplementary Figure 7:** Cell cycle based epistasis scores between NUDIX genes in CCD841, MCF7 and SW480 cells. The interaction maps visualize interactions determined based on the fraction of pairwise siRNA depleted cells in the cell cycle distribution. The panels show one interaction map per cell cycle phase. For each cell cycle phase, an interaction was assigned to a pair of genes if the cell fraction of the double knockdown was significantly different from the cell fraction of the double knockdown that would be expected if the genes were not interacting. The expected cell fraction was determined with a multiplicative null function. The interaction maps include negative (or decrease in cell fraction) interactions in brown, as well as positive (or increase in cell fraction) interactions in green. Positive interactions suggest that certain NUDIX product operate in concert or in series within the same pathway.

## CCD841 - Cell Cycle

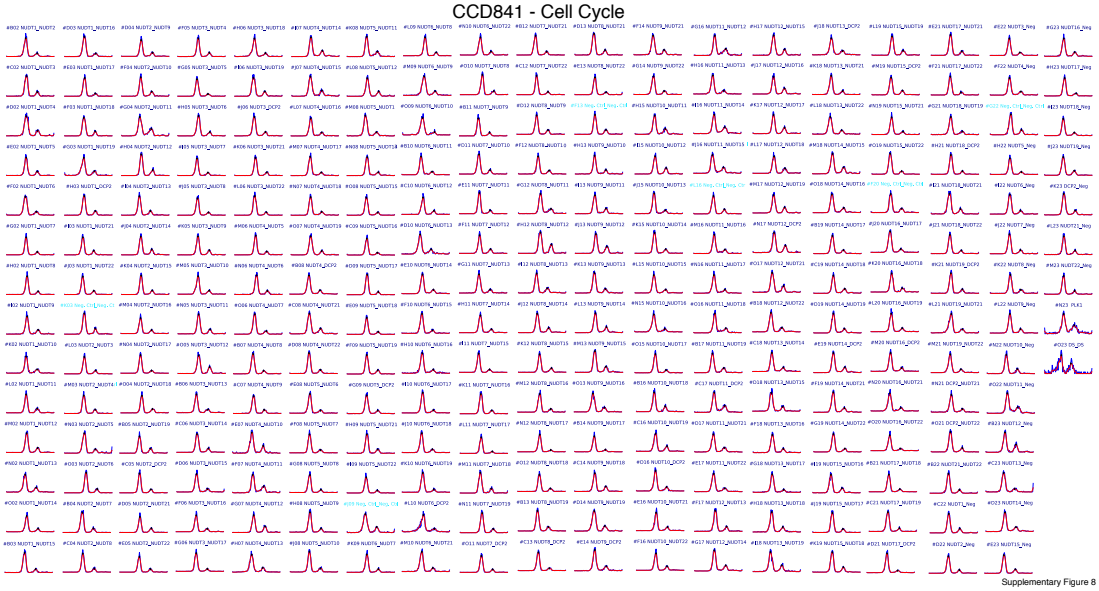

Supplementary Figure 8

## A549 - Cell Cycle

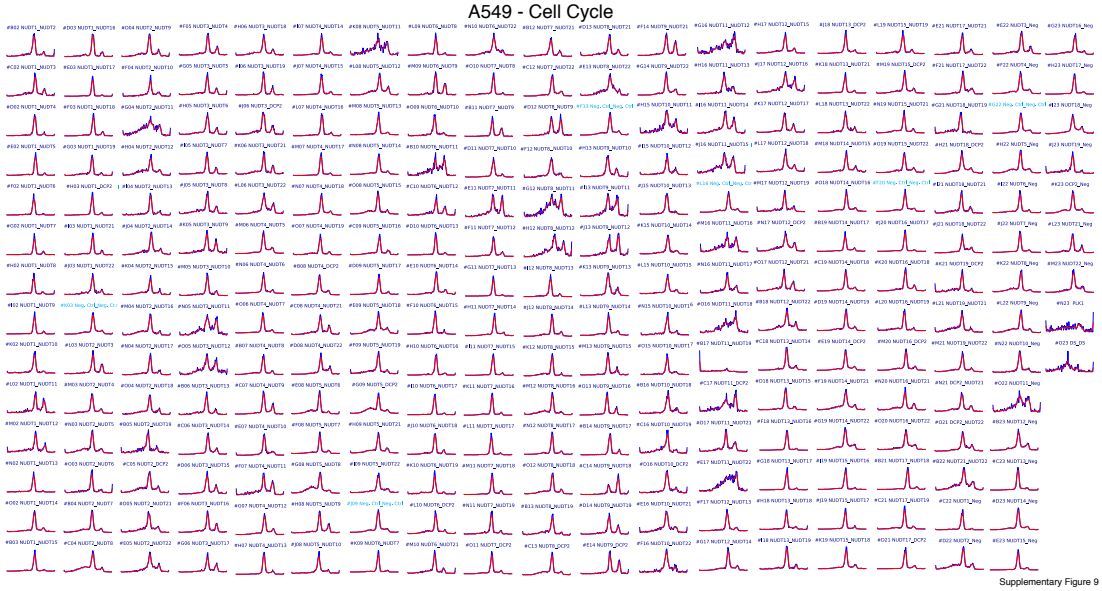

Supplementary Figure 9

## MCF7 - Cell Cycle

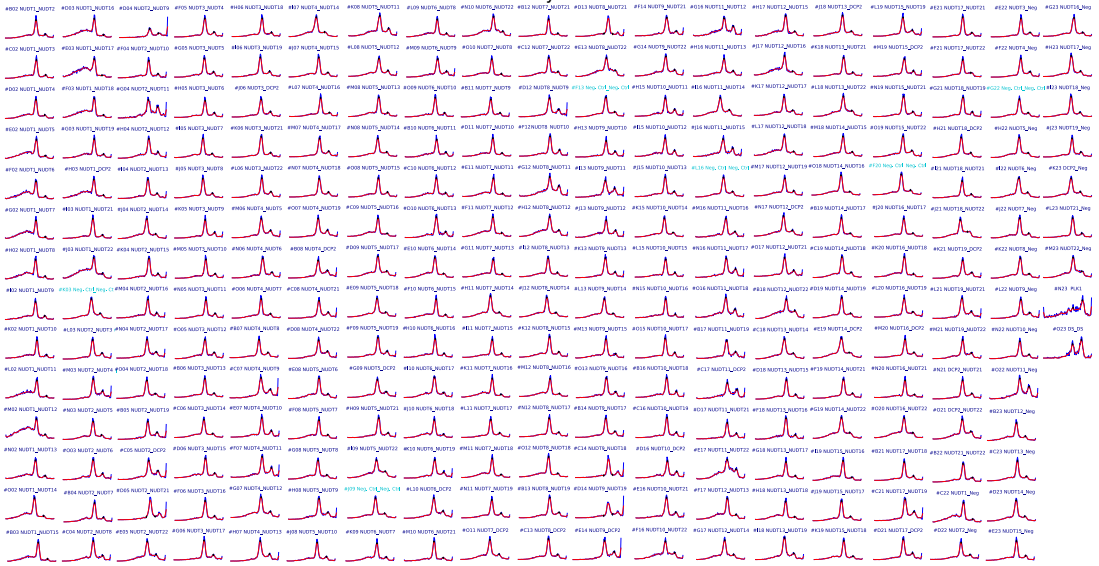

Supplementary Figure 10

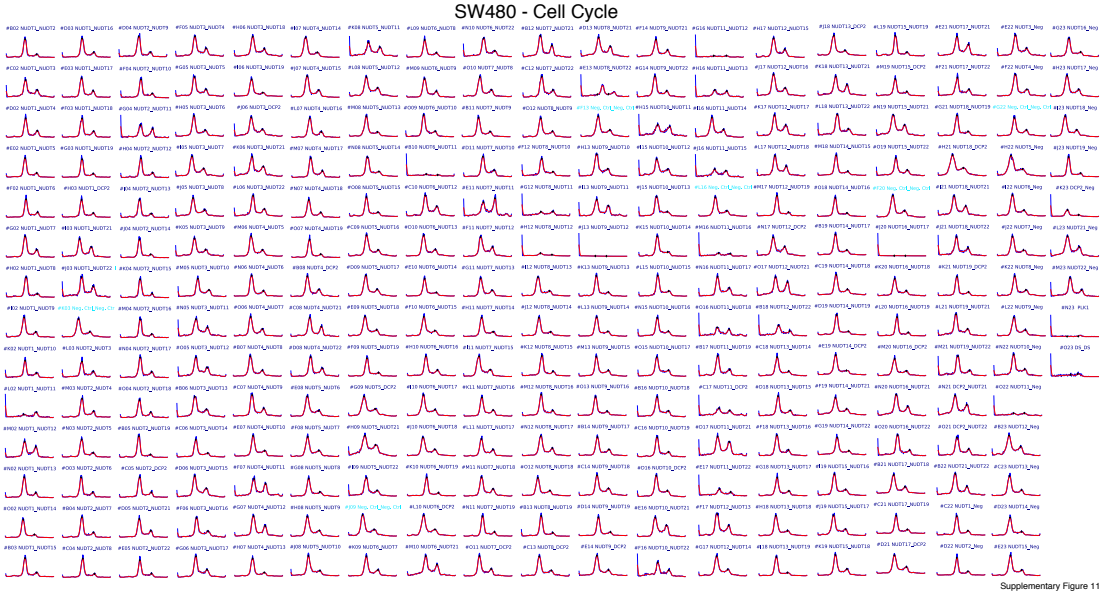


Supplementary Figure 11

**Supplementary Figures 8 to 11:** Cell cycle histograms of CCD841, A549, MCF7 and SW480 upon double NUDIX depletion. The graphical representation of the cell cycle histograms was obtained using PopulationProfiler.

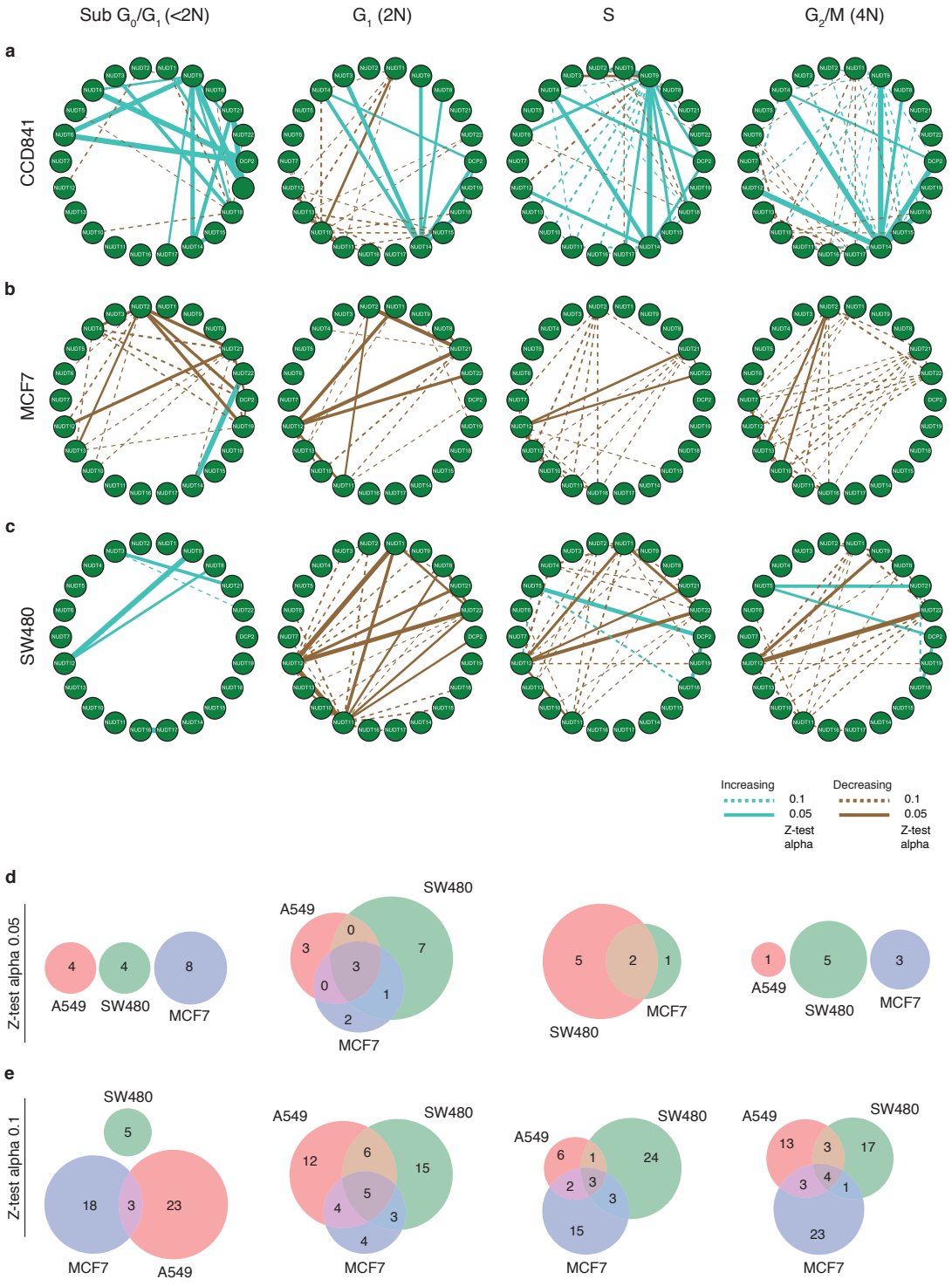


Supplementary Figure 12

**Supplementary Figure 12:** A to C: Selected cell cycle based interactions between NUDIX genes in CCD841, MCF7 and SW480 cells are visualized using circular networks. The panel shows one network per cell cycle phase. For each gene pair, the interaction was assessed by using a two-tailed Z test (indicated by a dotted line for alpha = 0.1, or solid line for alpha = 0.05). Shown are interactions whose values are significantly larger (positive

interaction with increase in cell fraction) in green, or significantly smaller (negative interaction with decrease in cell fraction) in brown, than values in the 90 % of interaction probability density. The interactions were selected independently and separately for each cell cycle phase in CCD841, MCF7 and SW480 cells. D and E: The overlap of significant genetic interactions from panels A, B and C is shown using Venn diagrams. The size of each circle in the diagram is proportional to the number of significant genetic interactions in the respective cell line.

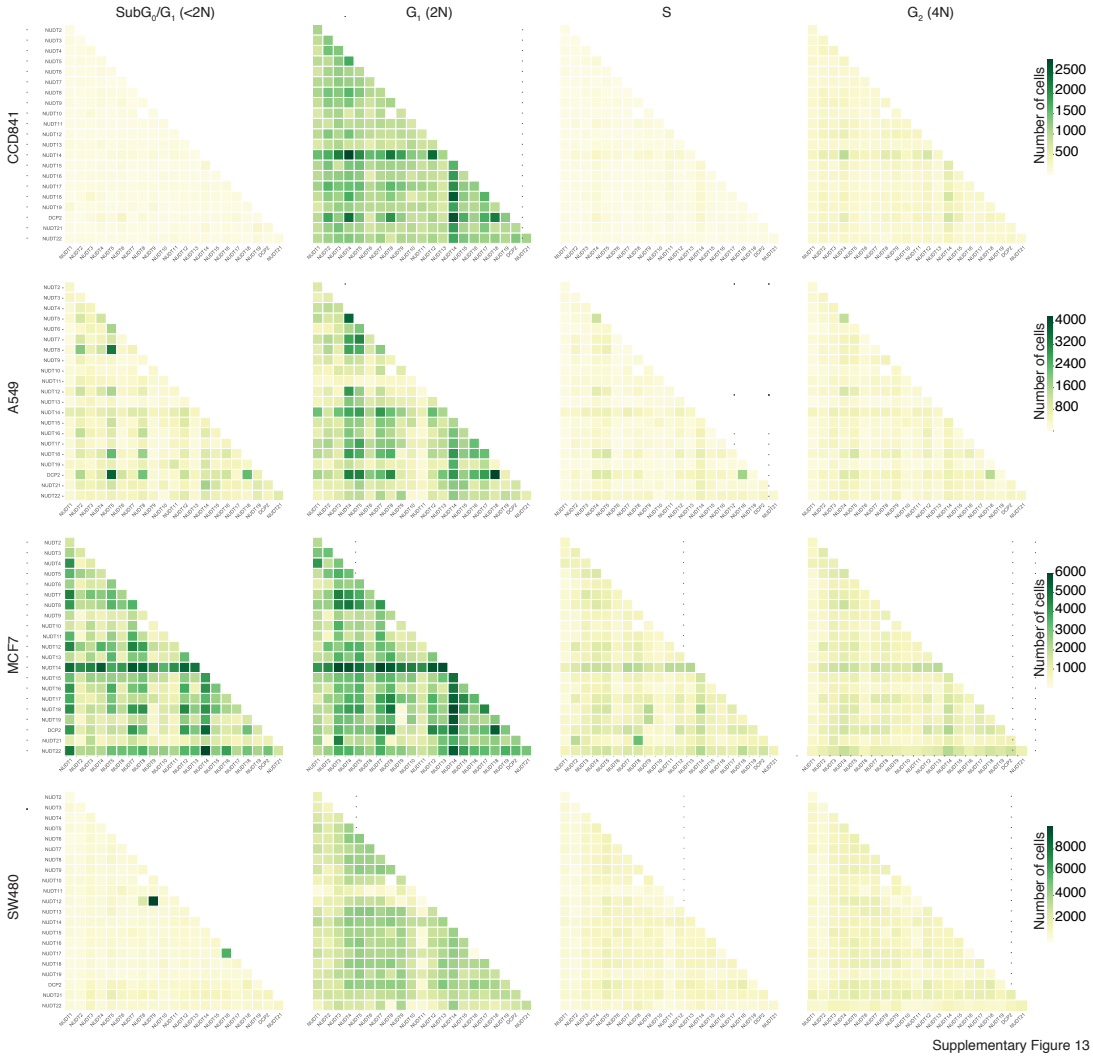


**Supplementary Figure 13**: Cell cycle distributions in double NUDIX knockdown. Heat map representations of the cell numbers in each cell cycle phase (<2N ($SubG_0/G_1$), 2N ($G_1$), S, 4N ($G_2$-M)) as determined using PopulationProfiler.

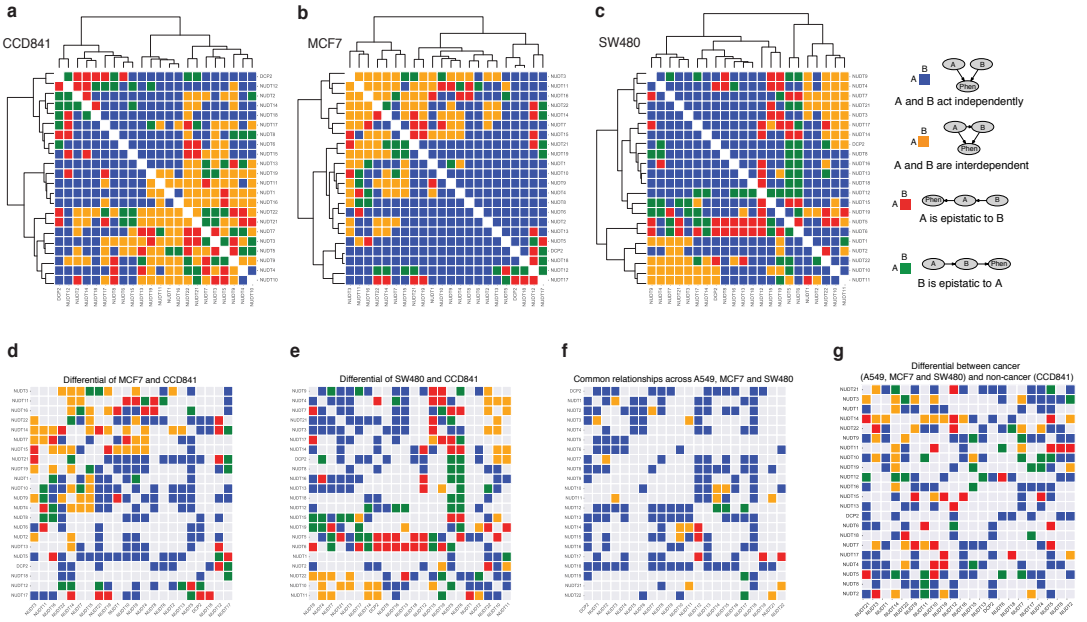


Supplementary Figure 14

**Supplementary Figure 14:** A, B and C: Many gene-gene relationships corresponding to independent activity in parallel pathways arise repeatedly when analysing knockdown phenotype data from different cancers. In addition to being interested in genetic relationships that persist across cancers we modelled cell viability data from individual cancer cell lines. D and E: Differential gene-gene relationships between MCF7, SW480 and CCD841, respectively. F: Common genetic interactions in all three cancer cell lines. G: Differential genetic interactions between all three cancer cell lines and the non-cancer cells CCD841. The space of cancer-specific gene-gene relationships shows substantial deviation from the space of corresponding relationships estimated from non-cancer cell data

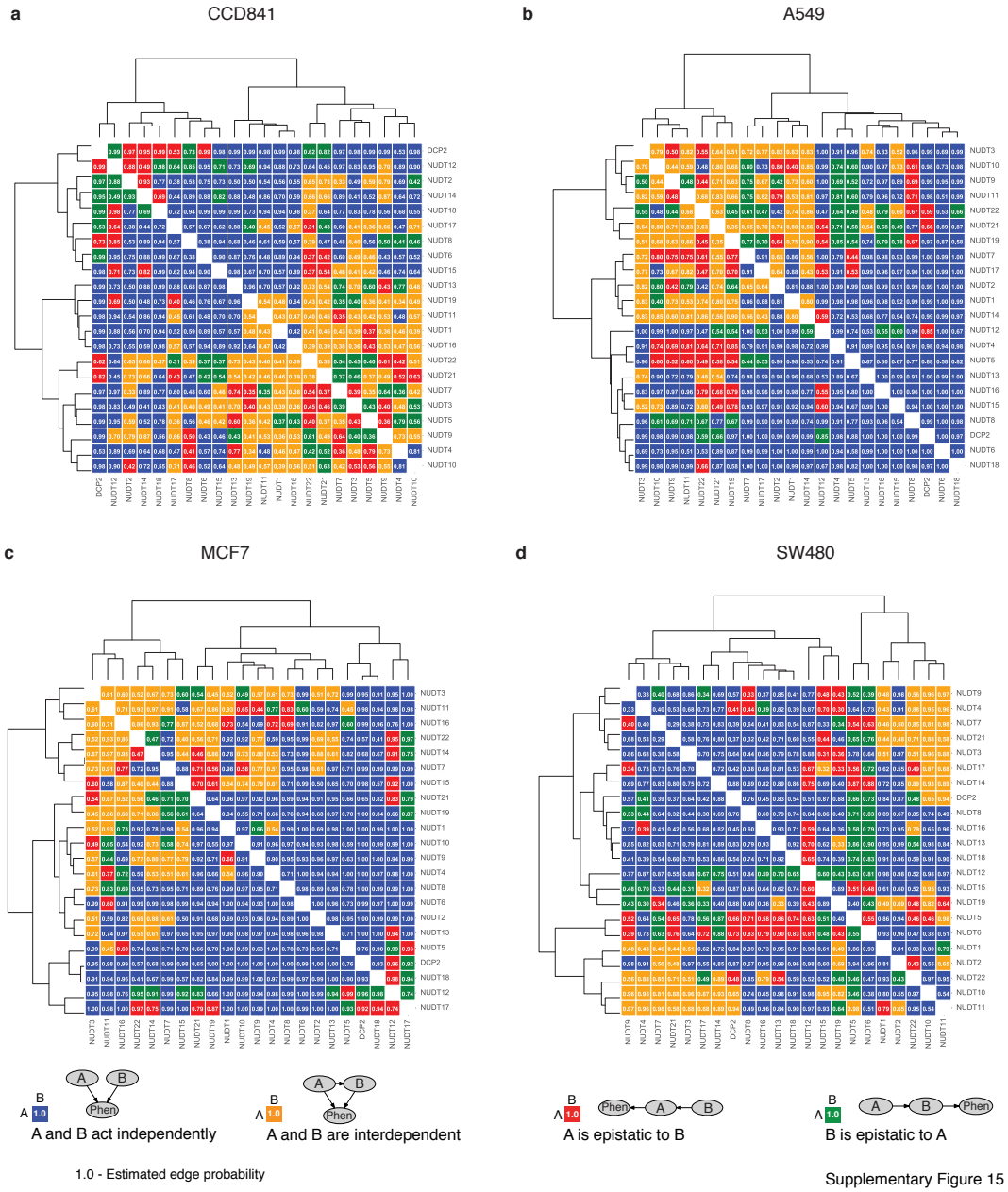


Supplementary Figure 15

**Supplementary Figure 15:** Probabilistic scoring of relationships from data on cell viability of single and double NUDIX knockdowns. We fed cell line-specific cell viability data to Réd and estimated probabilistic scores that predicted different types of pairwise NUDIX gene relationships. Prediction of gene-gene relationships involves estimating probabilities for four types of interaction, which are colour-coded in the figure: upstream epistasis, downstream epistasis, parallel pathway and partial interdependence. For a given cell line and a NUDIX gene pair, we show a relationship that was estimated with the highest probability by Réd and was also stable under small data perturbation. Numbers in the heat maps are probabilistic estimates for these most likely relationships. We further performed a hierarchical clustering on the heat maps using the Hamming distance as a measure of discordance between estimated

gene interaction profiles. Rows and columns of the heat maps were reordered according to clustering results.

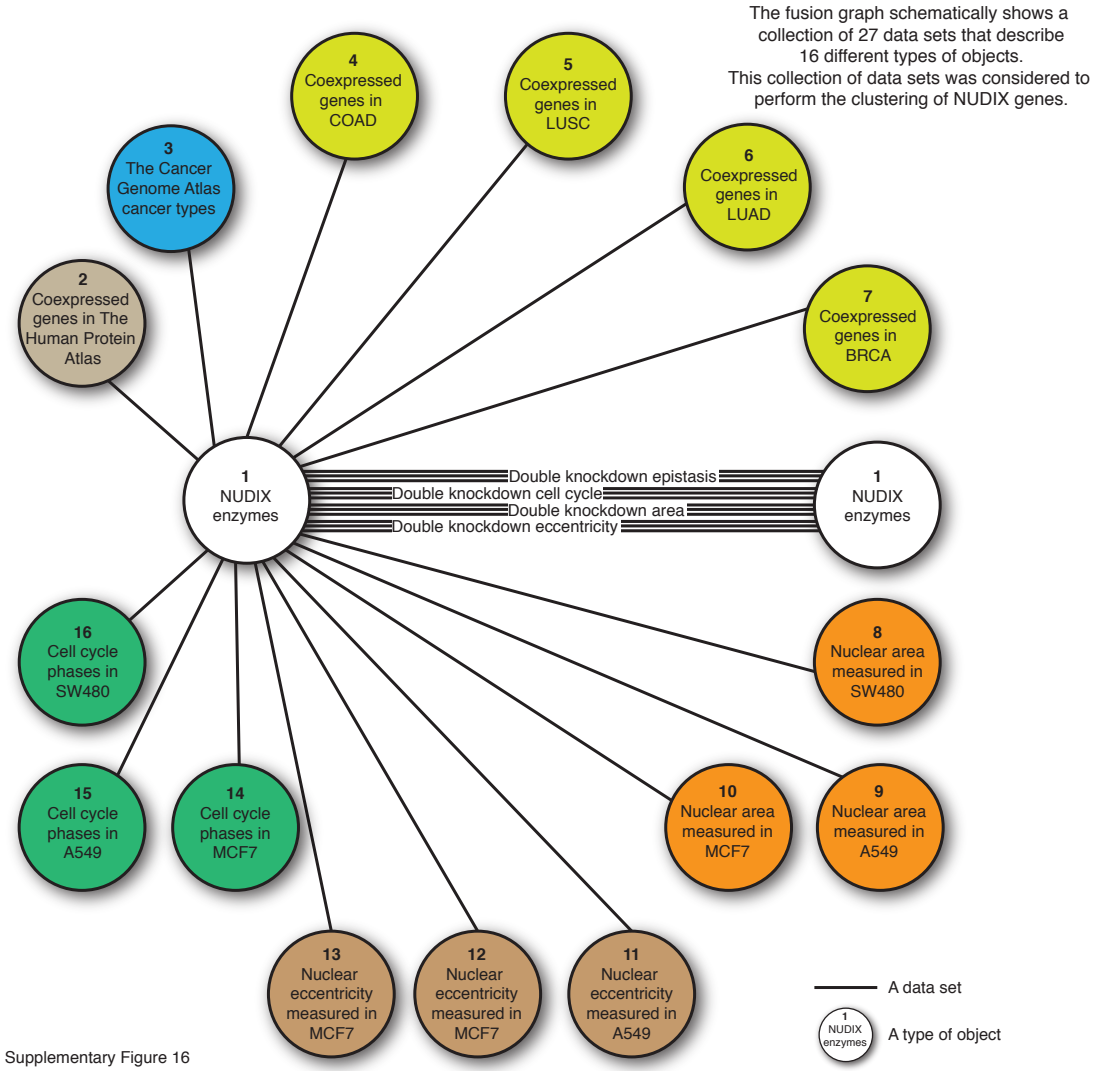


**Supplementary Figure 16**: Data fusion graph for mining data on NUDIX enzymes. The graph shows the organizational structure of data sets considered for our integrative clustering study. A node in the graph corresponds to a distinct object type. For example, the node named “The Cancer Genome Atlas cancer types” subsumes all cancer types from the TCGA (see Supplementary Data 2 - TCGA Cancer list and abbreviations), and node “Cell cycle phases in SW480” contains five phases of cell cycles, <2N ($SubG_0/G_1$), 2N ($G_1$), S, 4N ($G_2$-M). See Supplementary Data 3 for a detailed description of all data sets considered in the analysis. Edges in the graph correspond to data sets. The data fusion algorithm used to cluster NUDIX enzymes treats each data set as a data matrix, whose rows correspond to objects contained in one node of the respective edge and columns representing objects from the other node of the edge. For example, the edge from “NUDIX genes” to “Co-expressed genes in COAD” is technically a data matrix whose element in the *i*th row and *j*th column indicates the strength of co-expression between *i*th NUDIX gene and the *j*th gene in the TCGA COAD cancer type. To model data related to double

knockdowns we virtually doubled the “NUDIX genes” node while keeping its interacting data sets fixed. In total, our integrative data analysis considered 16 different object types and 27 different data sets.

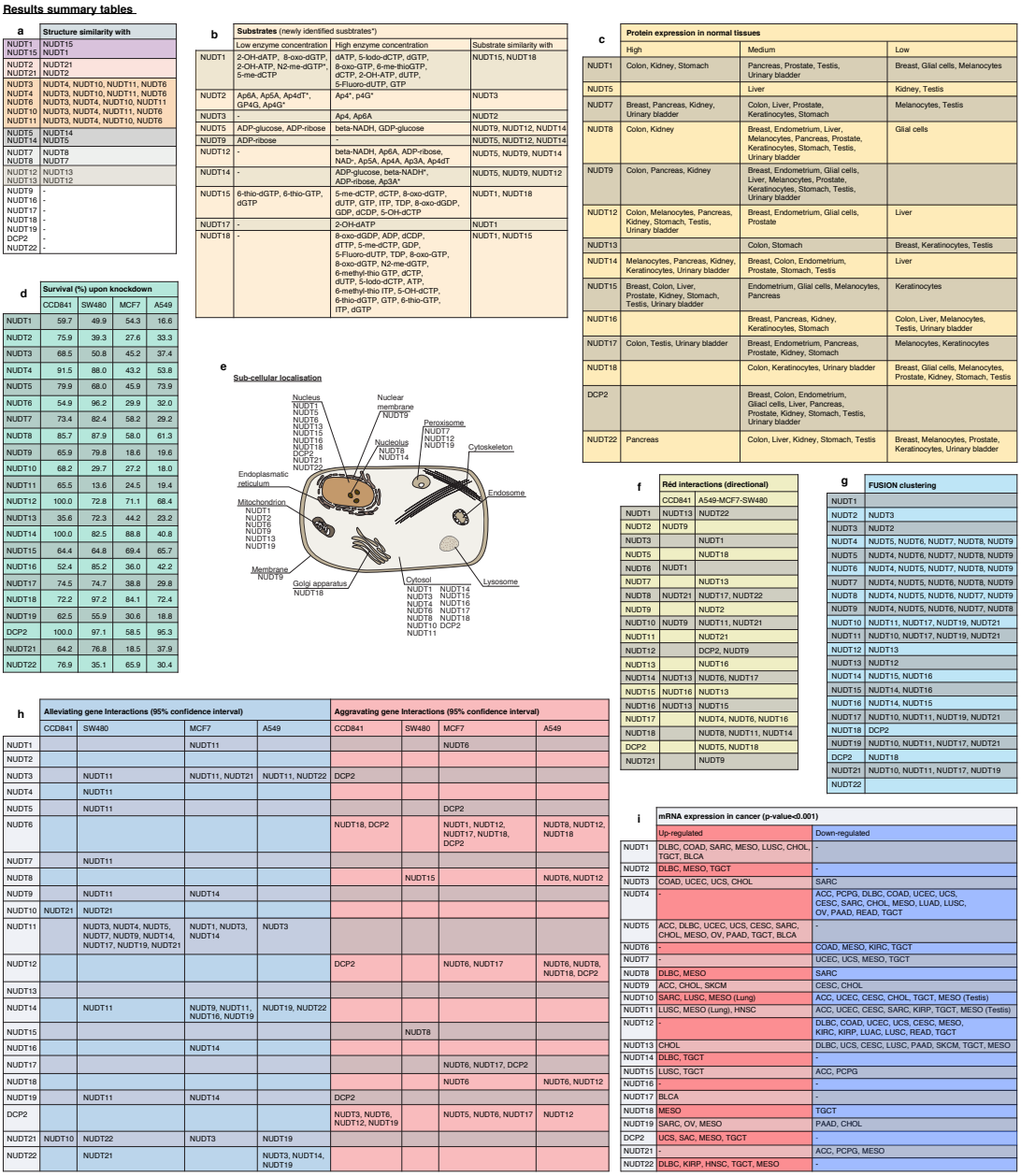

**Results summary tables**

**a**

| | Structure similarity with |
|---|---|
| NUDT1 | NUDT15 |
| NUDT15 | NUDT1 |
| NUDT2 | NUDT21 |
| NUDT21 | NUDT2 |
| NUDT3 | NUDT4, NUDT10, NUDT11, NUDT6 |
| NUDT4 | NUDT3, NUDT10, NUDT11, NUDT6 |
| NUDT6 | NUDT3, NUDT4, NUDT10, NUDT11 |
| NUDT10 | NUDT3, NUDT4, NUDT11, NUDT6 |
| NUDT11 | NUDT3, NUDT4, NUDT10, NUDT6 |
| NUDT5 | NUDT14 |
| NUDT14 | NUDT5 |
| NUDT7 | NUDT8 |
| NUDT8 | NUDT7 |
| NUDT12 | NUDT13 |
| NUDT13 | NUDT12 |
| NUDT9 | - |
| NUDT16 | - |
| NUDT17 | - |
| NUDT18 | - |
| NUDT19 | - |
| DCP2 | - |
| NUDT22 | - |

**b**

| | Substrates (newly identified susbtrates*) | | |
|---|---|---|---|
| | Low enzyme concentration | High enzyme concentration | Substrate similarity with |
| NUDT1 | 2-OH-dATP, 8-oxo-dGTP, 2-OH-ATP, N2-me-dGTP*, 5-me-dCTP | dATP, 5-Iodo-dCTP, dGTP, 8-oxo-GTP, 6-me-thioGTP, dCTP, 2-OH-ATP, dUTP, 5-Fluoro-dUTP, GTP | NUDT15, NUDT18 |
| NUDT2 | Ap6A, Ap5A, Ap4dT*, GP4G, Ap4G* | Ap4*, p4G* | NUDT3 |
| NUDT3 | - | Ap4, Ap6A | NUDT2 |
| NUDT5 | ADP-glucose, ADP-ribose | beta-NADH, GDP-glucose | NUDT9, NUDT12, NUDT14 |
| NUDT9 | ADP-ribose | - | NUDT5, NUDT12, NUDT14 |
| NUDT12 | - | beta-NADH, Ap6A, ADP-ribose, NAD+, Ap5A, Ap4A, Ap3A, Ap4dT | NUDT5, NUDT9, NUDT14 |
| NUDT14 | - | ADP-glucose, beta-NADH*, ADP-ribose, Ap3A* | NUDT5, NUDT9, NUDT12 |
| NUDT15 | 6-thio-dGTP, 6-thio-GTP, dGTP | 5-me-dCTP, dCTP, 8-oxo-dGTP, dUTP, GTP, ITP, TDP, 8-oxo-dGDP, GDP, dCDP, 5-OH-dCTP | NUDT1, NUDT18 |
| NUDT17 | - | 2-OH-dATP | NUDT1 |
| NUDT18 | - | 8-oxo-dCDP, ADP, dCDP, dTTP, 5-me-dCTP, GDP, 5-Fluoro-dUTP, TDP, 8-oxo-GTP, 8-oxo-dGTP, N2-me-dGTP, 6-methyl-thio GTP, dCTP, dUTP, 5-Iodo-dCTP, ATP, 6-methyl-thio ITP, 5-OH-dCTP, 6-thio-dGTP, GTP, 6-thio-GTP, ITP, dGTP | NUDT1, NUDT15 |

**c**

| | Protein expression in normal tissues | | |
|---|---|---|---|
| | High | Medium | Low |
| NUDT1 | Colon, Kidney, Stomach | Pancreas, Prostate, Testis, Urinary bladder | Breast, Glial cells, Melanocytes |
| NUDT5 | | Liver | Kidney, Testis |
| NUDT7 | Breast, Pancreas, Kidney, Urinary bladder | Colon, Liver, Prostate, Keratinocytes, Stomach | Melanocytes, Testis |
| NUDT8 | Colon, Kidney | Breast, Endometrium, Liver, Melanocytes, Pancreas, Prostate, Keratinocytes, Stomach, Testis, Urinary bladder | Glial cells |
| NUDT9 | Colon, Pancreas, Kidney | Breast, Endometrium, Glial cells, Liver, Melanocytes, Prostate, Keratinocytes, Stomach, Testis, Urinary bladder | |
| NUDT12 | Colon, Melanocytes, Pancreas, Kidney, Stomach, Testis, Urinary bladder | Breast, Endometrium, Glial cells, Prostate | Liver |
| NUDT13 | | Colon, Stomach | Breast, Keratinocytes, Testis |
| NUDT14 | Melanocytes, Pancreas, Kidney, Keratinocytes, Urinary bladder | Breast, Colon, Endometrium, Prostate, Stomach, Testis | Liver |
| NUDT15 | Breast, Colon, Liver, Prostate, Kidney, Stomach, Testis, Urinary bladder | Endometrium, Glial cells, Melanocytes, Pancreas | Keratinocytes |
| NUDT16 | | Breast, Pancreas, Kidney, Keratinocytes, Stomach | Colon, Liver, Melanocytes, Testis, Urinary bladder |
| NUDT17 | Colon, Testis, Urinary bladder | Breast, Endometrium, Pancreas, Prostate, Kidney, Stomach | Melanocytes, Keratinocytes |
| NUDT18 | | Colon, Keratinocytes, Urinary bladder | Breast, Glial cells, Melanocytes, Prostate, Kidney, Stomach, Testis |
| DCP2 | | Breast, Colon, Endometrium, Glial cells, Liver, Pancreas, Prostate, Kidney, Stomach, Testis, Urinary bladder | |
| NUDT22 | Pancreas | Colon, Liver, Kidney, Stomach, Testis | Breast, Melanocytes, Prostate, Keratinocytes, Urinary bladder |

**d**

| | Survival (%) upon knockdown | | | |
|---|---|---|---|---|
| | CCD841 | SW480 | MCF7 | A549 |
| NUDT1 | 59.7 | 49.9 | 54.3 | 16.6 |
| NUDT2 | 75.9 | 39.3 | 27.6 | 33.3 |
| NUDT3 | 68.5 | 50.8 | 45.2 | 37.4 |
| NUDT4 | 91.5 | 88.0 | 43.2 | 53.8 |
| NUDT5 | 79.9 | 68.0 | 45.9 | 73.9 |
| NUDT6 | 54.9 | 96.2 | 29.9 | 32.0 |
| NUDT7 | 73.4 | 82.4 | 58.2 | 29.2 |
| NUDT8 | 85.7 | 87.9 | 58.0 | 61.3 |
| NUDT9 | 65.9 | 79.8 | 18.6 | 19.6 |
| NUDT10 | 68.2 | 29.7 | 27.2 | 18.0 |
| NUDT11 | 65.5 | 13.6 | 24.5 | 19.4 |
| NUDT12 | 100.0 | 72.8 | 71.1 | 68.4 |
| NUDT13 | 35.6 | 72.3 | 44.2 | 23.2 |
| NUDT14 | 100.0 | 82.5 | 88.8 | 40.8 |
| NUDT15 | 64.4 | 64.8 | 69.4 | 65.7 |
| NUDT16 | 52.4 | 85.2 | 36.0 | 42.2 |
| NUDT17 | 74.5 | 74.7 | 38.8 | 29.8 |
| NUDT18 | 72.2 | 97.2 | 84.1 | 72.4 |
| NUDT19 | 62.5 | 55.9 | 30.6 | 18.8 |
| DCP2 | 100.0 | 97.1 | 58.5 | 95.3 |
| NUDT21 | 64.2 | 76.8 | 18.5 | 37.9 |
| NUDT22 | 76.9 | 35.1 | 65.9 | 30.4 |

**e**

**Sub-cellular localisation**



**f**

| | Réd interactions (directional) | |
|---|---|---|
| | CCD841 | A549-MCF7-SW480 |
| NUDT1 | NUDT13 | NUDT22 |
| NUDT2 | NUDT9 | |
| NUDT3 | | NUDT1 |
| NUDT5 | | NUDT18 |
| NUDT6 | NUDT1 | |
| NUDT7 | | NUDT13 |
| NUDT8 | NUDT21 | NUDT17, NUDT22 |
| NUDT9 | | NUDT2 |
| NUDT10 | NUDT9 | NUDT11, NUDT21 |
| NUDT11 | | NUDT21 |
| NUDT12 | | DCP2, NUDT9 |
| NUDT13 | | NUDT16 |
| NUDT14 | NUDT13 | NUDT6, NUDT17 |
| NUDT15 | NUDT16 | NUDT13 |
| NUDT16 | NUDT13 | NUDT15 |
| NUDT17 | | NUDT4, NUDT6, NUDT16 |
| NUDT18 | | NUDT8, NUDT11, NUDT14 |
| DCP2 | | NUDT5, NUDT18 |
| NUDT21 | | NUDT9 |

**g**

| | FUSION clustering |
|---|---|
| NUDT1 | |
| NUDT2 | NUDT3 |
| NUDT3 | NUDT2 |
| NUDT4 | NUDT5, NUDT6, NUDT7, NUDT8, NUDT9 |
| NUDT5 | NUDT4, NUDT6, NUDT7, NUDT8, NUDT9 |
| NUDT6 | NUDT4, NUDT5, NUDT7, NUDT8, NUDT9 |
| NUDT7 | NUDT4, NUDT5, NUDT6, NUDT8, NUDT9 |
| NUDT8 | NUDT4, NUDT5, NUDT6, NUDT7, NUDT9 |
| NUDT9 | NUDT4, NUDT5, NUDT6, NUDT7, NUDT8 |
| NUDT10 | NUDT11, NUDT17, NUDT19, NUDT21 |
| NUDT11 | NUDT10, NUDT17, NUDT19, NUDT21 |
| NUDT12 | NUDT13 |
| NUDT13 | NUDT12 |
| NUDT14 | NUDT15, NUDT16 |
| NUDT15 | NUDT14, NUDT16 |
| NUDT16 | NUDT14, NUDT15 |
| NUDT17 | NUDT10, NUDT11, NUDT19, NUDT21 |
| NUDT18 | DCP2 |
| NUDT19 | NUDT10, NUDT11, NUDT17, NUDT21 |
| DCP2 | NUDT18 |
| NUDT21 | NUDT10, NUDT11, NUDT17, NUDT19 |
| NUDT22 | |

**h**

| | Alleviating gene Interactions (95% confidence interval) | | | | Aggravating gene Interactions (95% confidence interval) | | | |
|---|---|---|---|---|---|---|---|---|
| | CCD841 | SW480 | MCF7 | A549 | CCD841 | SW480 | MCF7 | A549 |
| NUDT1 | | | NUDT11 | | | | NUDT6 | |
| NUDT2 | | | | | | | | |
| NUDT3 | | NUDT11 | NUDT11, NUDT21 | NUDT11, NUDT22 | DCP2 | | | |
| NUDT4 | | NUDT11 | | | | | | |
| NUDT5 | | NUDT11 | | | | | DCP2 | |
| NUDT6 | | | | | NUDT18, DCP2 | | NUDT1, NUDT12, NUDT17, NUDT18, DCP2 | NUDT8, NUDT12, NUDT18 |
| NUDT7 | | NUDT11 | | | | | | |
| NUDT8 | | | | | | NUDT15 | | NUDT6, NUDT12 |
| NUDT9 | | NUDT11 | NUDT14 | | | | | |
| NUDT10 | NUDT21 | NUDT21 | | | | | | |
| NUDT11 | | NUDT3, NUDT4, NUDT5, NUDT7, NUDT9, NUDT14, NUDT17, NUDT19, NUDT21 | NUDT1, NUDT3, NUDT14 | NUDT3 | | | | |
| NUDT12 | | | | | DCP2 | | NUDT6, NUDT17 | NUDT6, NUDT8, NUDT18, DCP2 |
| NUDT13 | | | | | | | | |
| NUDT14 | | NUDT11 | NUDT9, NUDT11, NUDT16, NUDT19 | NUDT19, NUDT22 | | | | |
| NUDT15 | | | | | | NUDT8 | | |
| NUDT16 | | | NUDT14 | | | | | |
| NUDT17 | | | | | | | NUDT6, NUDT17, DCP2 | |
| NUDT18 | | | | | | | NUDT6 | NUDT6, NUDT12 |
| NUDT19 | | NUDT11 | NUDT14 | | DCP2 | | | |
| DCP2 | | | | | NUDT3, NUDT6, NUDT12, NUDT19 | | NUDT5, NUDT6, NUDT17 | NUDT12 |
| NUDT21 | NUDT10 | NUDT22 | NUDT3 | NUDT19 | | | | |
| NUDT22 | | NUDT21 | | NUDT3, NUDT14, NUDT19 | | | | |

**i**

| | mRNA expression in cancer (p-value<0.001) | |
|---|---|---|
| | Up-regulated | Down-regulated |
| NUDT1 | DLBC, COAD, SARC, MESO, LUSC, CHOL, TGCT, BLCA | - |
| NUDT2 | DLBC, MESO, TGCT | - |
| NUDT3 | COAD, UCEC, UCS, CHOL | SARC |
| NUDT4 | - | ACC, PCPG, DLBC, COAD, UCEC, UCS, CESC, SARC, CHOL, MESO, LUAD, LUSC, OV, PAAD, READ, TGCT |
| NUDT5 | ACC, DLBC, UCEC, UCS, CESC, SARC, CHOL, MESO, OV, PAAD, TGCT, BLCA | - |
| NUDT6 | - | COAD, MESO, KIRC, TGCT |
| NUDT7 | - | UCEC, UCS, MESO, TGCT |
| NUDT8 | DLBC, MESO | SARC |
| NUDT9 | ACC, CHOL, SKCM | CESC, CHOL |
| NUDT10 | SARC, LUSC, MESO (Lung) | ACC, UCEC, CESC, CHOL, TGCT, MESO (Testis) |
| NUDT11 | LUSC, MESO (Lung), HNSC | ACC, UCEC, CESC, SARC, KIRP, TGCT, MESO (Testis) |
| NUDT12 | - | DLBC, COAD, UCEC, UCS, CESC, MESO, KIRC, KIRP, LUAC, LUSC, READ, TGCT |
| NUDT13 | CHOL | DLBC, UCS, CESC, LUSC, PAAD, SKCM, TGCT, MESO |
| NUDT14 | DLBC, TGCT | - |
| NUDT15 | LUSC, TGCT | ACC, PCPG |
| NUDT16 | - | - |
| NUDT17 | BLCA | - |
| NUDT18 | MESO | TGCT |
| NUDT19 | SARC, OV, MESO | PAAD, CHOL |
| DCP2 | UCS, SAC, MESO, TGCT | - |
| NUDT21 | - | ACC, PCPG, MESO |
| NUDT22 | DLBC, KIRP, HNSC, TGCT, MESO | - |

Supplementary Figure 17

**Supplementary Figure 17**: Results summary tables for each of the datasets obtained in our study. A: Structure similarity. B: Substrate activity. C: Protein expression in normal tissues. D: Survival upon siRNA-meditated knockdown. E: Sub-cellular localisation. F: Genetic interactions inferred by Réd. G: Clusters determined by FUSION. H: Alleviating or Aggravating epistatic interactions and I: mRNA expression in cancer (TCGA).

## Supplementary Tables

| Normal tissue | Tumor |
|---|---|
| Adrenal gland | Adrenocortical carcinoma |
| | Pheochromocytoma and Paraganglioma |
| Bone marrow | Acute Myeloid Leukemia |
| | Lymphoid Neoplasm Diffuse Large B-cell Lymphoma |
| Brain (cerebral cortex) | Brain Lower Grade Glioma |
| | Glioblastoma multiforme |
| Colon | Colon adenocarcinoma |
| Duodenum | Colon adenocarcinoma |
| Endometrium | Uterine Corpus Endometrial Carcinoma |
| | Uterine Carcinosarcoma |
| | Cervical squamous cell carcinoma and endocervical adenocarcinoma |
| Adipose tissue | Sarcoma |
| Gall bladder | Cholangiocarcinoma |
| Heart muscle | Mesothelioma |
| Kidney | Kidney renal clear cell carcinoma |
| | Kidney renal papillary cell carcinoma |
| Liver | Liver hepatocellular carcinoma |
| Lung | Lung adenocarcinoma |
| | Lung squamous cell carcinoma |
| | Mesothelioma |
| Lymphnode | Lymphoid Neoplasm Diffuse Large B-cell Lymphoma |
| Ovary | Ovarian serous cystadenocarcinoma |
| Pancreas | Pancreatic adenocarcinoma |
| | Cholangiocarcinoma |
| Prostate | Prostate adenocarcinoma |
| Rectum | Rectal adenocarcinoma |
| Salivary gland | Head and Neck squamous cell carcinoma |
| Skeletal muscle | Sarcoma |
| Skin | Skin Cutaneous Melanoma |
| Smooth muscle | Sarcoma |
| Testis | Testicular Germ Cell Tumors |
| | Mesothelioma |
| Thyroid | Thyroid carcinoma |
| Urinary bladder | Bladder Urothelial carcinoma |

**Supplementary Table 1:** Pairwise comparisons between normal tissues and tumors. This pairing was used to match normal and cancer tissues for the analysis of TCGA and HPA sequencing data.

| Data set | Data set position in the fusion graph | Data set description | Data set size |
|---|---|---|---|
| R(1,2) | R(NUDIX genes, genes in the HPA) | Spearman rank correlation measurements of mRNA coexpression in the HPA data | 22x978 |
| R(1,3) | R(NUDIX genes, TCGA cancer projects) | mRNA expression in cancer tissues taken from the TCGA database | 22x29 |
| R(1,4) | R(NUDIX genes, genes in the COAD cohort) | Spearman rank correlation measurements of mRNA coexpression in the COAD cohort | 22x1891 |
| R(1,5) | R(NUDIX genes, genes in the LUSC cohort) | Spearman rank correlation measurements of mRNA coexpression in the LUSC cohort | 22x141 |
| R(1,6) | R(NUDIX genes, genes in the LUAD cohort) | Spearman rank correlation measurements of mRNA coexpression in the LUAD cohort | 22x335 |
| R(1,7) | R(NUDIX genes, genes in the BRCA cohort) | Spearman rank correlation measurements of mRNA coexpression in the BRCA cohort | 22x909 |
| R(1,8) | R(NUDIX genes, measurements of area in SW480 cells) | Cell area of single siRNA knockdowns in the SW480 cells obtained with Cell Profiler software | 22x100 |
| R(1,9) | R(NUDIX genes, measurements of area in A549 cells) | Cell area of single siRNA knockdowns in the A549 cells obtained with Cell Profiler software | 22x100 |
| R(1,10) | R(NUDIX genes, measurements of area in MCF7 cells) | Cell area of single siRNA knockdowns in the MCF7 cells obtained with Cell Profiler software | 22x100 |
| R(1,11) | R(NUDIX genes, measurements of eccentricity in A549 cells) | Cell eccentricity of single siRNA knockdowns in the A549 cells obtained with Cell Profiler software | 22x100 |
| R(1,12) | R(NUDIX genes, measurements of eccentricity in MCF7 cells) | Cell eccentricity of single siRNA knockdowns in the MCF7 cells obtained with Cell Profiler software | 22x100 |
| R(1,13) | R(NUDIX genes, measurements of eccentricity in SW480 cells) | Cell eccentricity of single siRNA knockdowns in the SW480 cells obtained with Cell Profiler software | 22x100 |
| R(1,14) | R(NUDIX genes, measurements of cell cycle in MCF7 cells) | Counts of single siRNA knockdown cells in the MCF7 across cell cycle phases <2N, 2N, S, 4N, >4N obtained with Cell Profiler software | 22x5 |
| R(1,15) | R(NUDIX genes, | Counts of single siRNA knockdown | 22x5 |

| | | | |
|---|---|---|---|
| | measurements of cell cycle in A549 cells) | cells in the A549 across cell cycle phases <2N, 2N, S, 4N, >4N obtained with Cell Profiler software | |
| R(1,16) | R(NUDIX genes, measurements of cell cycle in SW480 cells) | Counts of single siRNA knockdown cells in the SW480 across cell cycle phases <2N, 2N, S, 4N, >4N obtained with Cell Profiler software | 22x5 |
| R(1,1) | R(NUDIX genes, NUDIX genes) | Cell area of double siRNA knockdowns in the A549 cells obtained with Cell Profiler software | 22x22x100 |
| R(1,1) | R(NUDIX genes, NUDIX genes) | Cell area of double siRNA knockdowns in the SW480 cells obtained with Cell Profiler software | 22x22x100 |
| R(1,1) | R(NUDIX genes, NUDIX genes) | Cell area of double siRNA knockdowns in the MCF7 cells obtained with Cell Profiler software | 22x22x100 |
| R(1,1) | R(NUDIX genes, NUDIX genes) | Cell eccentricity of double siRNA knockdowns in the A549 cells obtained with Cell Profiler software | 22x22x100 |
| R(1,1) | R(NUDIX genes, NUDIX genes) | Cell eccentricity of double siRNA knockdowns in the SW480 cells obtained with Cell Profiler software | 22x22x100 |
| R(1,1) | R(NUDIX genes, NUDIX genes) | Cell eccentricity of double siRNA knockdowns in the MCF7 cells obtained with Cell Profiler software | 22x22x100 |
| R(1,1) | R(NUDIX genes, NUDIX genes) | Counts of double siRNA knockdown cells in the A549 across cell cycle phases <2N, 2N, S, 4N, >4N obtained with Cell Profiler software | 22x22x5 |
| R(1,1) | R(NUDIX genes, NUDIX genes) | Counts of double siRNA knockdown cells in the SW480 across cell cycle phases <2N, 2N, S, 4N, >4N obtained with Cell Profiler software | 22x22x5 |
| R(1,1) | R(NUDIX genes, NUDIX genes) | Counts of double siRNA knockdown cells in the MCF7 across cell cycle phases <2N, 2N, S, 4N, >4N obtained with Cell Profiler software | 22x22x5 |
| R(1,1) | R(NUDIX genes, NUDIX genes) | Epistasis score of interaction in the A549 cells | 22x22 |
| R(1,1) | R(NUDIX genes, NUDIX | Epistasis score of interaction in the | 22x22 |

| | | | |
|---|---|---|---|
| | genes) | SW480 cells | |
| R(1,1) | R(NUDIX genes, NUDIX genes) | Epistasis score of interaction in the MCF7 cells | 22x22 |

| **Color legend** | |
|---|---|
| | Data from the MCF7 human breast cancer cells |
| | Data from the A549 human lung cancer/adenocarcinoma cells |
| | Data from the SW480 human colon adenocarcinoma cells |
| | Data not specific to any individual cancer tissue or cell line |

**Supplementary Table 2:** List of data sets used for clustering the human NUDIX family.

| Cancer name | Abbreviation. |
|---|---|
| Adrenocortical carcinoma | ACC |
| Bladder Urothelial Carcinoma | BLCA |
| Breast invasive carcinoma | BRCA |
| Cervical squamous cell carcinoma and endocervical adenocarcinoma | CESC |
| Cholangiocarcinoma | CHOL |
| Colon adenocarcinoma | COAD |
| Lymphoid Neoplasm Diffuse Large B-cell Lymphoma | DLBC |
| Glioblastoma multiforme | GBM |
| Head and Neck squamous cell carcinoma | HNSC |
| Kidney renal clear cell carcinoma | KIRC |
| Kidney renal papillary cell carcinoma | KIRP |
| Acute Myeloid Leukemia | LAML |
| Brain Lower Grade Glioma | LGG |
| Liver hepatocellular carcinoma | LIHC |
| Lung adenocarcinoma | LUAD |
| Lung squamous cell carcinoma | LUSC |
| Mesothelioma | MESO |
| Ovarian serous cystadenocarcinoma | OV |
| Pancreatic adenocarcinoma | PAAD |
| Pheochromocytoma and Paraganglioma | PCPG |
| Prostate adenocarcinoma | PRAD |
| Rectum adenocarcinoma | READ |
| Sarcoma | SARC |
| Skin Cutaneous Melanoma | SKCM |
| Testicular Germ Cell Tumors | TGCT |
| Thyroid carcinoma | THCA |
| Uterine Corpus Endometrial Carcinoma | UCEC |
| Uterine Carcinosarcoma | UCS |
| Uveal Melanoma | UVM |

**Supplementary Table 3:** TCGA cancer types abbreviations.

| Gene | Distributor | Product code | Species | Dilution | Ensembl Gene ID |
|---|---|---|---|---|---|
| MTH1/ NUDT1 | Atlas Antibodies AB | HPA012636 | Rabbit | 300 | ENSG00000106268 |
| NUDT5 | Atlas Antibodies AB | HPA019827 | Rabbit | 250 | ENSG00000165609 |
| NUDT7 | Atlas Antibodies AB | HPA042042 | Rabbit | 35 | ENSG00000140876 |
| NUDT8 | Atlas Antibodies AB | HPA041466 | Rabbit | 250 | ENSG00000167799 |
| NUDT9 | Atlas Antibodies AB | HPA044866 | Rabbit | 3000 | ENSG00000170502 |
| NUDT12 | Atlas Antibodies AB | HPA045449 | Rabbit | 800 | ENSG00000112874 |
| NUDT13 | Atlas Antibodies AB | HPA040636 | Rabbit | 35 | ENSG00000166321 |
| NUDT14 | Atlas Antibodies AB | HPA046755 | Rabbit | 150 | ENSG00000183828 |
| NUDT15 | Atlas Antibodies AB | HPA038969 | Rabbit | 1250 | ENSG00000136159 |
| NUDT16 | Atlas Antibodies AB | HPA060452 | Rabbit | 15 | ENSG00000198585 |
| NUDT17 | Atlas Antibodies AB | HPA030145 | Rabbit | 500 | ENSG00000186364 |
| NUDT18 | Atlas Antibodies AB | HPA028581 | Rabbit | 10 | ENSG00000275074 |
| NUDT22 | Atlas Antibodies AB | HPA039334 | Rabbit | 40 | ENSG00000149761 |
| DCP2 | Abcam plc | ab28658 | Rabbit | 35 | ENSG00000172795 |

**Supplementary Table 4:** List of antibodies used for TMA and IHC.

| Gene Symbol | GENE ID | Gene Accession | siRNA Sequence |
|---|---|---|---|
| NUDT1 | 4521 | NM_002452 | GACGACAGCUACUGGUUUC |
| NUDT1 | 4521 | NM_002452 | GAAAUUCCACGGGUACUUC |
| NUDT1 | 4521 | NM_002452 | CGACGACAGCUACUGGUUU |
| NUDT1 | 4521 | NM_002452 | AGACGUGGCUGCUGAACAG |
| NUDT2 | 318 | NM_001161 | GAGGGAGACCCAAGAGGAA |
| NUDT2 | 318 | NM_001161 | GAGCAUGUGGCUUGAUCAU |
| NUDT2 | 318 | NM_001161 | UUCCCAAAGUGGACAACAA |
| NUDT2 | 318 | NM_001161 | GAAGAUGCCUCAUUCCCAA |
| NUDT3 | 11165 | NM_006703 | GCACAGGACGUAUGUCUAU |
| NUDT3 | 11165 | NM_006703 | GAAGGAAGAGGGAAUGGUU |
| NUDT3 | 11165 | NM_006703 | UAAAAGUGCUGCAGUAUCA |
| NUDT3 | 11165 | NM_006703 | UGAGGAGGCUGGAGUAAAA |
| NUDT4 | 11163 | NM_019094 | GGAUAAUAAUGCCUUGUUU |
| NUDT4 | 11163 | NM_019094 | GAAUGGAACCCGAGGAGGA |
| NUDT4 | 11163 | NM_019094 | CGAAAGCACAGAACAUAUG |
| NUDT4 | 11163 | NM_019094 | GGGUUGCCAUCUAGUGUAA |
| NUDT5 | 11164 | NM_014142 | GCAGAGAACACUUCACUAU |
| NUDT5 | 11164 | NM_014142 | GGCAAACAGUAUAUCAUUU |
| NUDT5 | 11164 | NM_014142 | CAGAGGAGUUAAUUUCAGA |
| NUDT5 | 11164 | NM_014142 | GAACUUGGGAAUCAGUGAA |
| NUDT6 | 11162 | NM_007083 | GAAGAAUGCUUAAGAUGUG |
| NUDT6 | 11162 | NM_007083 | GAACUGCCAGAGAAUUAUA |
| NUDT6 | 11162 | NM_007083 | UAUAUCAUCUGCCGCCUAA |
| NUDT6 | 11162 | NM_007083 | CCAUAUUCAUUCACCAUAA |
| NUDT7 | 283927 | NM_001105663 | GUAUGAUAUUGGAGGCAAA |
| NUDT7 | 283927 | NM_001105663 | UCAAGGGAAUGACGGCAAA |
| NUDT7 | 283927 | NM_001105663 | ACAAAGAACUAUUCACGAG |
| NUDT7 | 283927 | NM_001105663 | GCCAUGUCUUAUUGAUACA |
| NUDT8 | 254552 | NM_181843 | GCACAAGGGCGACGUCAGU |
| NUDT8 | 254552 | NM_181843 | GGUGUAGGCCCACUGGAUC |
| NUDT8 | 254552 | NM_181843 | ACUCGGAGGAGGUGAGCUG |
| NUDT8 | 254552 | NM_181843 | CUGUGUAUGAUCCGCAAAA |
| NUDT9 | 53343 | NM_024047 | GGAAGCAUAUCUUACAAUU |
| NUDT9 | 53343 | NM_024047 | GAAGCCAGGUUCCUAAUGA |
| NUDT9 | 53343 | NM_024047 | GAACUACCAUGACGAAACA |
| NUDT9 | 53343 | NM_024047 | GGAUAGCAGUGGAAAUAAA |
| NUDT10 | 170685 | NM_153183 | GCACAGAACGUACGUGUAU |
| NUDT10 | 170685 | NM_153183 | GACGAGGUCCUGUUAGUGA |
| NUDT10 | 170685 | NM_153183 | CGCCGAAUAUCUGGAGAAA |
| NUDT10 | 170685 | NM_153183 | GUGCAAACCCAACCAGACA |
| NUDT11 | 55190 | NM_018159 | CCGAAUAUCUGGAGAAACU |
| NUDT11 | 55190 | NM_018159 | GCACAGAACGUACGUGUAU |
| NUDT11 | 55190 | NM_018159 | GGGAAGAUUCGGUUAGCAU |
| NUDT11 | 55190 | NM_018159 | GGAGCGAACGCGAGGACGA |
| NUDT12 | 83594 | NM_031438 | CAUAAUACCUCAUACCCAA |
| NUDT12 | 83594 | NM_031438 | GGUUGUAGCUCAAGCAAGA |
| NUDT12 | 83594 | NM_031438 | GGAGAUAUUGCCAAGUUAA |
| NUDT12 | 83594 | NM_031438 | GGAAAGUGGAGUCAAAGUU |
| NUDT13 | 25961 | NM_015901 | GCACAAAGAAUAGAAGAUU |

| | | | |
|---|---|---|---|
| NUDT13 | 25961 | NM_015901 | UGGAAAGGCUCCUGGGUAA |
| NUDT13 | 25961 | NM_015901 | GGAAUAGCUUGCAGGAGAA |
| NUDT13 | 25961 | NM_015901 | CAACCUAUGUUACUAAGAC |
| NUDT14 | 256281 | NM_177533 | GGACGGGCCUCGGGAGCUA |
| NUDT14 | 256281 | NM_177533 | UGGAGGAAGUGGCUUGCAA |
| NUDT14 | 256281 | NM_177533 | GGAGCCUGGUGUUGGUGAA |
| NUDT14 | 256281 | NM_177533 | AGACAGACCAUGUUCUACA |
| NUDT15 | 55270 | NM_018283 | GGAUGUGACUCAUGAUUCA |
| NUDT15 | 55270 | NM_018283 | ACAAGGCUAUGAUCCAUUU |
| NUDT15 | 55270 | NM_018283 | GGAGAAUUACCAUUAUGUU |
| NUDT15 | 55270 | NM_018283 | CAUCUGGAGUUCGGUGAAA |
| NUDT16 | 131870 | NM_152395 | GCUGCAGUCUGGCUCUAUU |
| NUDT16 | 131870 | NM_152395 | CUACCUUCCUGGAGAAUUC |
| NUDT16 | 131870 | NM_152395 | CUGUAUACCCUGCGGGAUG |
| NUDT16 | 131870 | NM_152395 | CCUUAAGAUUCCAGCUCAU |
| NUDT17 | 200035 | NM_001012758 | UCUGGAAAGUGAAGUGUAA |
| NUDT17 | 200035 | NM_001012758 | GGACGGAGGGCUUCGAGAA |
| NUDT17 | 200035 | NM_001012758 | CAACCUUUAUUAUGGGUGA |
| NUDT17 | 200035 | NM_001012758 | GUUUAUGGGAGUCUGCCUA |
| NUDT18 | 79873 | NM_024815 | GUGGAAUUCUCAAGACUUC |
| NUDT18 | 79873 | NM_024815 | GAGCUACCCUGUGAUCUGG |
| NUDT18 | 79873 | NM_024815 | GCAAGAGGCUGGCGAUCAG |
| NUDT18 | 79873 | NM_024815 | GCACGUUGCUGAGUAAAGA |
| NUDT19 | 390916 | NM_001105570 | UAAGAACUCUGUAGUAAGA |
| NUDT19 | 390916 | NM_001105570 | UGAGAAGACUUGCAAACUU |
| NUDT19 | 390916 | NM_001105570 | GACAUACCAUCGCCACCUU |
| NUDT19 | 390916 | NM_001105570 | CCACGUGACUGUUCAGCCA |
| DCP2 | 167227 | NM_152624 | GAAAUUGCCUUGUCAUAGA |
| DCP2 | 167227 | NM_152624 | GAUAAGAGACUUUGCUAAA |
| DCP2 | 167227 | NM_152624 | GAAGAGAAAUUCGGAACAU |
| DCP2 | 167227 | NM_152624 | GGAAACUUCAGGAUAAUUU |
| NUDT21 | 11051 | NM_007006 | GCGCAUGAGGGAAGAAUUU |
| NUDT21 | 11051 | NM_007006 | CUAAGGAACAUAAGAAGUU |
| NUDT21 | 11051 | NM_007006 | UGACAAUGCACCAGGAUAU |
| NUDT21 | 11051 | NM_007006 | ACGCUUAAUGACAGAGAUA |
| NUDT22 | 84304 | NM_032344 | CCACGAGUCUACAGGAAUC |
| NUDT22 | 84304 | NM_032344 | GCCGAUGACUUCCUUGUCU |
| NUDT22 | 84304 | NM_032344 | ACACAGAACGUGCGGAGAU |
| NUDT22 | 84304 | NM_032344 | GAGCCAGUGCCGAGUUCUA |

| **Gene Symbol house keeping genes** | **qRT-PCR primer sequence 5'-3'** |
|---|---|
| hGAPDH forward | AAGGTCGGAGTCAACGGATT |
| hGAPDH reverse | CTCCTGGAAGATGGTGATGG |
| Beta Actin forward | CCTGGCACCCAGCACAAT |
| Beta Actin reverse | GGCCGGACTCGTCATACT |

| **Gene Symbol** | **GENE ID** | **Gene Accession** | **qRT-PCR primer sequence 5'-3'** |
|---|---|---|---|
| NUDT1 forward | 4521 | NM_002452.3 | GGTGCAGAACCCAGGGAC |
| NUDT1 reverse | 4521 | NM_002452.3 | CTTTGCCCCCAAAGCCATTC |
| NUDT2 forward | 318 | NM_001161.4 | TTTCTGCCTCAACCACGGAC |

| | | | |
|---|---|---|---|
| NUDT2 reverse | 318 | NM_001161.4 | CAAACGCACCCATTCCAGAAG |
| NUDT3 forward | 11165 | NM_006703.3 | AGCTCAAGTCGAACCAGACC |
| NUDT3 reverse | 11165 | NM_006703.3 | TCACGAGTAGCACCTCCTCC |
| NUDT4 forward | 4521 | NM_002452 | CCAGTGGATTGTCCCAGGAG |
| NUDT4 reverse | 4521 | NM_002452 | GGTCTTGGTTCTCAAATATGCCC |
| NUDT5 forward | 11164 | NM_014142 | ATCCTTTTAGCACCGCGAGA |
| NUDT5 reverse | 11164 | NM_014142 | CAGGTGAGAAGTTCACCTCCAA |
| NUDT6 forward | 11162 | NM_007083 | GTAGGAGTTGCAGGAGCTGT |
| NUDT6 reverse | 11162 | NM_007083 | CTTCTCGAACCGCTGTGTCT |
| NUDT7 forward | 283927 | NM_001105663 | CCGTCCTTTTGCCATTGGTG |
| NUDT7 reverse | 283927 | NM_001105663 | GGGGCCCTTCTTAGCTTCTC |
| NUDT8 forward | 254552 | NM_181843 | CCCAACTCGGAGGAGGTAGA |
| NUDT8 reverse | 254552 | NM_181843 | CCATGCAGGAAGACGGGTAG |
| NUDT9 forward | 53343 | NM_024047 | ACCTAGCATCGCAAAGCCG |
| NUDT9 reverse | 53343 | NM_024047 | ACGAGTTTCTGAACGCCTGG |
| NUDT10 forward | 170685 | NM_153183.2 | CGTGCCACACACCTCGG |
| NUDT10 reverse | 170685 | NM_153183.2 | TGTCTGGTTGGGTTTGCACT |
| NUDT11 forward | 55190 | NM_018159.3 | AGCGATCCCTAATGAACAGCA |
| NUDT11 reverse | 55190 | NM_018159.3 | TGGGAACACAGAAGTGCTCA |
| NUDT12 forward | 83594 | NM_031438.2 | CTGTGGTCACCTTTGGGAAGA |
| NUDT12 reverse | 83594 | NM_031438.2 | GGCAATATCTCCTTCAGCAGC |
| NUDT13 forward | 25961 | NM_015901.5 | AGCCGTTGAACGTGAACATTT |
| NUDT13 reverse | 25961 | NM_015901.5 | TCTCCTGCAAGCTATTCCACA |
| NUDT14 forward | 256281 | NM_177533.4 | CATTACCGCCAGAATGGTGC |
| NUDT14 reverse | 256281 | NM_177533.4 | GGCTCCTCCGAGAAGAGTTG |
| NUDT15 forward | 55270 | NM_018283.1 | GGAAGAGGAAAGGCTCGGTT |
| NUDT15 reverse | 55270 | NM_018283.1 | CCCAGGTTTCACCGAACTCC |
| NUDT16 forward | 131870 | NM_001171906.1 | GTGCCACGCTCTCCTCTAC |
| NUDT16 reverse | 131870 | NM_001171906.1 | GCATCTGCATCAGTATGGCG |
| NUDT17 forward | 200035 | NM_001012758.2 | GAGTGTGTGTGGCCTCCTG |
| NUDT17 reverse | 200035 | NM_001012758.2 | AGAAAGGGGGTCGCTGGA |
| NUDT18 forward | 79873 | NM_024815.3 | GGCTGCGGAAGAACGTGT |
| NUDT18 reverse | 79873 | NM_024815.3 | GATCAGTAGCACCTCATCCTGC |
| NUDT19 forward | 390916 | NM_001105570.1 | CTCACCCCTTTCTTGCGGG |
| NUDT19 reverse | 390916 | NM_001105570.1 | CTGATGGAGATGACCACTGGTAG |
| NUDT20 forward | 167227 | NM_152624.5 | CTGACGGTTCTCCTGGTGAC |
| NUDT20 reverse | 167227 | NM_152624.5 | TCCCCTCATACTTTGATTCTTTCCT |
| NUDT21 forward | 11051 | NM_007006.2 | GCACCATCAACCTGTACCCT |
| NUDT21 reverse | 11051 | NM_007006.2 | CTCATGCGCTGAAATCTGGC |

**Supplementary Table 5:** List of siRNA sequences used for the depletion of all the NUDIX genes, and list of qRT-PCR primers used to determine NUDIX mRNA levels.

**Supplementary Note:**

**Methodology remarks**

The methodologies used in this work are a combination of well-established approaches as well as innovative bioinformatics analyses. Despite our careful assessment, execution and interpretation of experiments and results, there are limitations to take into consideration.

The outcome of the structural analysis based on phylogeny may vary depending on the method applied, indeed, the combination of Markov chain Monte Carlo (MCMC) and Bayesian algorithms, gave the most statistically robust phylogenetic tree, which differed from other methods, thus a careful choice of method is of utmost importance.

We used the Malachite Green assay to determine substrate activity for the 18 NUDIX enzymes that we analysed. Given the large diversity of substrates and enzymes, the conditions in which the highest hydrolase activity is achieved are equally diverse. We opted for a unified condition in the presence of magnesium and a constant pH of 7.5, which may have limited the efficiency of the reactions, therefore limiting the number of identified substrates. The limitations of single point substrate activity assays are to be considered, as well as the relevancy of such assessments regarding the availability of the chosen substrates in the cell, as recently reported[1], since the concentration of the identified substrates may, in some cases, be considerably lower in cells than the concentration used in our substrate screen. Also, the concentration

of the individual NUDIX proteins in the cell is not known, hence, our results should serve as a basis for more in depth functional studies of this family of proteins. The complete lack of activity observed for some NUDIX hydrolases may indicate the need of specific reaction conditions and/or absence of their substrates in the tested panel. For example, NUDT10 and NUDT11 may require manganese as divalent cation instead of magnesium as has been previously suggested[2]. Another possibility is that the His-tag, present on all of our purified NUDIX proteins, in some cases may negatively affect the enzyme activity. Finally, murine NUDT7 has been shown to hydrolyse Coenzyme A[3], an activity we could not reproduce. The lack of activity of NUDT6 and NUDT21 is consistent with earlier publications[4, 5]

The TCGA as well as the Human Protein Atlas databases contain a plethora of valuable data, however to make use of it, especially when comparing datasets from two different databases, strict normalizations need to be made. Our normalized data clearly indicates differences among the different NUDIX at mRNA and protein levels, in both cancer and normal tissues, however, the experimental conditions in which these measurements have been made may condition the results, thus individual validation may be advisable for further studies.

Despite the risk of potential off-target effects, small interference RNAs are widely used for the transient depletion of target genes. We used this approach to evaluate the viability of the studied cell lines in the absence of the NUDIX enzymes, as well as to investigate potential epistatic relationships among these. We evaluated the overall knockdown efficiency by qPCR and statistically compared two independent single siRNA-mediated depletion experiments, which highly correlated, validating our approach. However, it is important to note that the potential epistatic interactions could be masked by inefficient knockdown in a given population of cells. For epistasis analysis, we considered single and double knockdown viability measurements, and for a pair of NUDIX enzymes, we analysed whether a change in the first gene

masked the effects of a knockdown in the second gene. We used the multiplicative model to calculate the expected viability of a double knockdown in the absence of a genetic interaction. Although the multiplicative model is an established approach to define genetic interaction and was previously used in many large-scale genetic interactions studies, other mathematically distinct definitions of genetic interactions are possible, including the additive and logarithmic definitions. We thus report quantitative viability measurements of single and double NUDIX knockdowns to allow reclassification of interactions under any definition of genetic interaction.

To infer the order of function of the NUDIX enzymes in molecular pathways that are active in different cell lines we used a probabilistic approach to epistasis-based gene network inference. This approach, called Réd, allowed us to assemble a NUDIX gene network in each cell line based on probabilistic scoring of gene relationships measured in that cell line. Previous *in-silico* analyses showed that Réd can accurately reconstruct known gene pathways, is robust to noise and measurement errors, and that it outperforms current methods for gene network reconstruction. However, inference of gene networks requires solving a complicated non-convex optimization problem and current optimization techniques can only find a local mathematical optimum of the optimization problem through application of gradient descent algorithms. We thus performed additional computational experiments and sensitivity analyses to test the inferred gene networks and to validate their robustness to small data perturbations and to variation of optimization parameters.

Our integrative analyses used the FUSION algorithm to cluster NUDIX enzymes based on joint consideration of 27 datasets. The considered datasets are heterogeneous, differ in scale and range of values, and contain diverse measurements to describe qualitatively different phenomena relevant to the NUDIX enzymes. Therefore our analysis involved careful normalization of each dataset and its representation with a data matrix, followed by an

application of the machine learning algorithm FUSION, that inferred a predictive latent model, and clustering of the NUDIX enzymes based on the inferred model. To test the quality of the inferred model we tracked the progress of optimization implemented in the FUSION algorithm. We validated the results by experimentally interrogating selected NUDIX clusters identified by the FUSION algorithm, performing siRNA-mediated depletion of the NUDIX genes assigned to a given cluster, and evaluated the effect on expression of the rest of the NUDIX enzymes present in the cluster by qPCR.

Obtaining the sub-cellular localization of each NUDIX was not an objective of this work, for this we referred to the publicly available databases Human Protein Atlas and UniProt. It is important to note that the information in these databases is updated as measurements become more accurate and information becomes available; therefore certain localisations here mentioned might be subjected to changes. Despite the potential specific drawbacks and limitations of each methodology, we have applied normalization approaches to minimize errors and variations, providing an overall high confidence in the herein presented results.

## References


1. Nguyen, V.N. *et al.* Substrate specificity characterization for eight putative nudix hydrolases. Evaluation of criteria for substrate identification within the Nudix family. *Proteins* **84**, 1810-1822 (2016).
2. Leslie, N.R., McLennan, A.G. & Safrany, S.T. Cloning and characterisation of hAps1 and hAps2, human diadenosine polyphosphate-metabolising Nudix hydrolases. *BMC Biochem.* **3**, 20 (2002).
3. Gasmi, L. & McLennan, A.G. The mouse Nudt7 gene encodes a peroxisomal nudix hydrolase specific for coenzyme A and its derivatives. *Biochem J* **357**, 33-38 (2001).
4. Baguma-Nibasheka, M., Li, A.W. & Murphy, P.R. The fibroblast growth factor-2 antisense gene inhibits nuclear accumulation of FGF-2 and delays

cell cycle progression in C6 glioma cells. *Mol Cell Endocrinol* **267**, 127-136 (2007).

5. Yang, Q., Gilmartin, G.M. & Doublie, S. Structural basis of UGUA recognition by the Nudix protein CFI(m)25 and implications for a regulatory role in mRNA 3' processing. *Proc Natl Acad Sci U S A* **107**, 10062-10067 (2010).